AD-A184 658 VISUALIZATION OF THE FLOW FIELD AROUND A GENERIC DESTROYER MODEL IN A SIM (U) NAVAL POSTGRADUATE SCHOOL MONTEREY CA W K BOLINGER JUN 87 1/1

UNCLASSIFIED F/G 20/4 NL

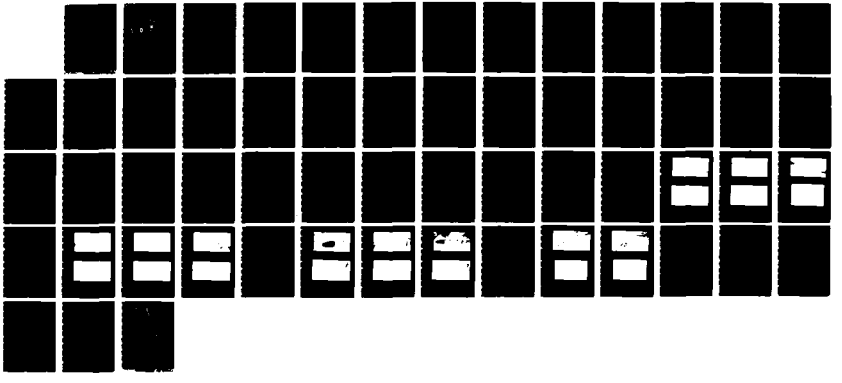

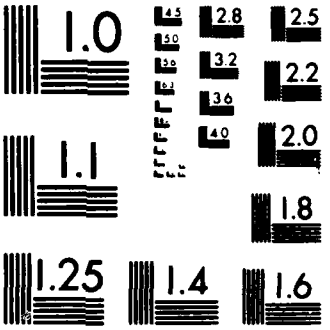

NAVAL POSTGRADUATE SCHOOL
Monterey, California

THESIS

VISUALIZATION OF THE FLOW FIELD AROUND A GENERIC DESTROYER MODEL IN A SIMULATED TURBULENT ATMOSPHERIC BOUNDARY LAYER

by

William K. Bolinger

June 1987

Thesis Advisor J. Val Healey

SECURITY CLASSIFICATION OF THIS PAGE

REPORT DOCUMENTATION PAGE

1a REPORT SECURITY CLASSIFICATION: UNCLASSIFIED	1b RESTRICTIVE MARKINGS
2a SECURITY CLASSIFICATION AUTHORITY	3 DISTRIBUTION/AVAILABILITY OF REPORT: Approved for public release; distribution is unlimited.
2b DECLASSIFICATION/DOWNGRADING SCHEDULE	
4 PERFORMING ORGANIZATION REPORT NUMBER(S)	5 MONITORING ORGANIZATION REPORT NUMBER(S)
6a NAME OF PERFORMING ORGANIZATION: Naval Postgraduate School; 6b OFFICE SYMBOL (If applicable): 67	7a NAME OF MONITORING ORGANIZATION: Naval Postgraduate School
6c ADDRESS (City, State, and ZIP Code): Monterey, California 93943-5000	7b ADDRESS (City, State, and ZIP Code): Monterey, California 93943-5000
8a NAME OF FUNDING/SPONSORING ORGANIZATION; 8b OFFICE SYMBOL (If applicable)	9 PROCUREMENT INSTRUMENT IDENTIFICATION NUMBER
8c ADDRESS (City, State, and ZIP Code)	10 SOURCE OF FUNDING NUMBERS: PROGRAM ELEMENT NO; PROJECT NO; TASK NO; WORK UNIT ACCESSION NO

11 TITLE (Include Security Classification): Visualization of the Flow Field around a Generic Destroyer model in a Simulated Turbulent Atmospheric Boundary Layer

12 PERSONAL AUTHOR(S): Bolinger, William K.

13a TYPE OF REPORT	13b TIME COVERED	14 DATE OF REPORT (Year Month Day)	15 PAGE COUNT
Master's Thesis	FROM ____ TO ____	1987 June	57

16 SUPPLEMENTARY NOTATION

17 COSATI CODES		
FIELD	GROUP	SUB-GROUP

18 SUBJECT TERMS (Continue on reverse if necessary and identify by block number): Flow Visualization, Atmospheric Boundary Layer, Fluorescent Minitufts, Helium Bubble

19 ABSTRACT (Continue on reverse if necessary and identify by block number)

An experimental flow visualization study was performed on a rectangular block and other elements that could be assembled in the form of a generic destroyer ship model in the Low Speed Flow Visualization Facility at the Naval Postgraduate School, Monterey, California. The purpose of the study was to visually analyze the flow field around the model in a simulated open ocean atmospheric boundary layer. To ensure correct simulation of the atmospheric boundary layer, both velocity profile and longitudinal turbulence intensities were matched.

For the actual flow visualization studies, two techniques were used. During the on-body portion of the study, the ultraviolet lighting/fluorescent minituft technique was used. For the off-body portion, helium bubble system, with a neutral density centrifuge, was utilized.

Both techniques produced excellent photographic results and allowed for

20 DISTRIBUTION/AVAILABILITY OF ABSTRACT	21 ABSTRACT SECURITY CLASSIFICATION
☒ UNCLASSIFIED/UNLIMITED ☐ SAME AS RPT ☐ DTIC USERS	unclassified

22a NAME OF RESPONSIBLE INDIVIDUAL	22b TELEPHONE (Include Area Code)	22c OFFICE SYMBOL
Healey, J. Val	408-646-2804	67He

DD FORM 1473, 84 MAR — 83 APR edition may be used until exhausted. All other editions are obsolete.

SECURITY CLASSIFICATION OF THIS PAGE

direct comparison of the flow fields using the two flow visualization techniques.

Approved for public release; distribution is unlimited.

Visualization of the Flow Field around a Generic Destroyer model in a Simulated Turbulent Atmospheric Boundary Layer

by

William Kelly Bolinger
Lieutenant Commander, United States Navy
B.S., University of Colorado, 1974
M.B.A.,Chapman College, 1980

Submitted in partial fulfillment of the requirements for the degree of

MASTERS OF SCIENCE IN AERONAUTICAL ENGINEERING

from the

NAVAL POSTGRADUATE SCHOOL
June 1987

Author : William K Bolinger
William K. Bolinger

Approved by : J Val Healey
J. Val Healey, Thesis Advisor

M. F. Platz
M.F. Platzer, Chairman, Department of Aeronautics

G E Schacher
G.E. Schacher, Dean of Science and Engineering

ABSTRACT

An experimental flow visualization study was performed on a rectangular block and other elements that could be assembled in the form of a generic destroyer ship model in the Low Speed Flow Visualization Facility at the Naval Postgraduate School, Monterey, California. The purpose of the study was to visually analyze the flow field around the model in a simulated open ocean atmospheric boundary layer. To ensure correct simulation of the atmospheric boundary layer, both velocity profile and longitudinal turbulence intensities were matched.

For the actual flow visualization studies, two techniques were used. During the on-body portion of the study, the ultraviolet lighting / fluorescent minituft technique was used. For the off-body portion, a helium bubble system, with a neutral density centrifuge, was utilized.

Both techniques produced excellent photographic results and allowed for direct comparison of the flow field using the two flow visualization techniques.

TABLE OF CONTENTS

TABLE OF CONTENTS (Cont)

LIST OF FIGURES

List of Figures (Cont)

ACKNOWLEDGEMENTS

Grateful acknowledgement is made to Professor J. Val Healey, of the Naval Postgraduate School Aeronautical Engineering Department, for his knowledgeable expertise and endless hours of support in the wind tunnel. Sincere appreciation is extended to Mr. Ron Ramaker, Naval Postgraduate School Aeronautical Engineering Modeling Technician, for his patience and quick reponses to the frequent changes in wind tunnel modifications.

My sincerest thanks to my loving wife, typist and editor, without whose full support this thesis would not have been possible. And, I am especially grateful to the Lord, who has blessed me with a sound mind and the fortitude required to see this project through to its completion.

I. INTRODUCTION

In recent times, a considerable effort has been ongoing to improve the United States Navy's flexibility by increasing the number of ships and helicopters authorized to conduct flight operations together. This increasing number and variety of helicopters operating with less traditional landing platforms can introduce unknown turbulent air wake problems during launch and recovery operations. These problems can then become critical to the helicopter when combined with high winds, rough seas, and pitching decks.

The purpose of this investigation was threefold. The first portion of the study was to determine if the Naval Postgraduate School's low speed smoke tunnel could be modified to produce a realistic open-ocean atmospheric boundary layer velocity profile with the required turbulence level. The second part was to investigate the off-body flow of a bluff body and a generic destroyer ship model in a realistic simulation of the open-ocean turbulent atmospheric boundary layer. This part was conducted using the helium bubble flow visualization technique. The final portion of the study was designed to investigate the on-body flow of the same models, using an ultraviolet fluorescent minituft system.

The required modifications to the low speed wind tunnel and the two flow visualization techniques are described in

detail in the following sections. In addition, a review of the atmospheric boundary layer and its pertinent properties is included in the simulation discussion. The experimental results are discussed and evaluated with recommendations for follow-on projects.

II. TURBULENT ATMOSPHERIC SIMULATION

The first part of the study involved the correct simulation of the lower portion of the open-ocean turbulent atmospheric boundary layer (ABL). Many published studies, including References 1 and 2, have indicated that it is not sufficient to model just the mean velocity profile when simulating the atmosphere. In Reference 1, Healey suggests that there are four important parameters:

i) The average windspeed over a period of time or the mean velocity;

ii) The standard deviation of the longitudinal (along-wind) windspeed fluctuations about the mean which, when divided by the mean velocity, is called turbulence intensity;

iii) The longitudinal length scale of the turbulence, or 'integral' length scale, which is a measure of the size of the strongest eddies in the turbulence; and

iv) The turbulence spectrum function, which indicates the energy distribution of the frequencies present in the turbulence.

Now, an exact duplication of all aspects of an ABL flow field at a smaller scale is not possible. However, simplifications are permitted due to the special nature of the ABL. To be exactly modeled, the reference length Lr, the reference velocity Vr, a reference time Tr, and a reference

temperature need to be matched for the model and prototype. As the first simplification, the flow is assumed to be stationary. Even though the velocity itself is time dependent, the statistics of the fluctuations are taken as independent of time. This is a realistic assumption in that most large scale unsteadiness in the ABL takes place gradually. The Strouhal numbers are relevant when any kind of frequency is involved. In the case of a stationary ship, there is no time dependent vortex shedding nor is the ship model oscillating. If it were, the Strouhal numbers must be equal for true similarty. Even when there is neither oscillating nor shedding, the frequencies of the turbulence in the atmosphere and tunnel are related through the Strouhal numbers. The neutral density ABL is an idealized form and results in a constant thickness layer in which Coriolis forces and pressure gradient maintain constant velocity and shear stress at a given elevation along the earth's surface. Thus, in a neutral density ABL, the Coriolis parameter and the Rossby number can be ignored.

One successful approach to developing a proper simulation was accomplished by Counihan in Reference 3. His basic approach was to use vortex generators to pull back the flow at lower levels to model the mean velocity profile, and roughness elements to model the low-level turbulence. The correct combination and matching between the vortex

generators and the roughness elements will then produce a velocity profile and shear stress, which adequately model the atmospheric flow.

A. THEORETICAL REQUIREMENTS FOR ATMOSPHERIC MODELING

Arya, in Chapter 6 of Reference 2, describes the ABL as a turbulent layer, which is a function of the interaction of friction, roughness height, thermal stratifications, and Coriolis forces. In the case of a neutral density boundary layer near the surface, where momentum flux is assumed to be constant, the well known logarithmic relationship leads to a wind velocity profile of,

$$\bar{U}/U_* = (1/K)\ln(Z/z_o) \qquad (1)$$

where $\bar{U}$ is the average velocity, U_* is the friction velocity, z_o is the roughness parameter, Z the vertical distance from the surface, and K is Von Karman's constant.

This equation should also be recognized as the 'Law of the Wall', which represents the airflow over a given surface. In Reference 4, Davenport further refines equation (1) by substituting Von Karman's constant and developing equation (2), the Power Law Velocity Profile,

$$\bar{U}/Ug = (Z/Zg)^n \qquad (2)$$

with Ug the gradient velocity and Zg the gradient height. Now, if the mean velocity is known at a given height,

then these values can be used instead of Ug and Zg in equation (2).

The table below, which is from Chapter 12 of Reference 4, shows values for n, using the Power Law Profile, and assumes the given values of z_o.

SURFACE	z_o (meters)	n	Zg (meters)
Sea	.001-.01	.11-.15	250
Prairie	.01-0.1	.16	300
Forest	0.1-1.0	.28	400

The Power Law Profile has been used in many engineering problems, and was used in this report to develop the ABL velocity profile. This profile matches very closely to the logarithmic profile form over a large range of values.

Turbulence arises from the instability of the rest states and laminar motions in the atmosphere. These instabilities are related to gradients in temperature, pressure, and velocity. In the ABL, where the turbulence is largely from ground or sea roughness, the most important parameter of the turbulence is the fluctuating longitudinal velocity component. The primary feature distinguishing one area of turbulence from another is the turbulence intensity, or root mean square (RMS) of the speed fluctuations. The turbulence

intensity parameter is then defined for the longitudinal direction as

$$Ti = RMS/\bar{U}. \qquad (3)$$

B. EXPERIMENTAL APPARATUS AND MEASUREMENTS

1. Wind Tunnel Description

The experiment was conducted in the low speed wind tunnel at the Naval Postgraduate School (NPS), Monterey, California. The low speed tunnel is essentially a three-dimensional smoke tunnel, as shown in Figure 1, modeled after the tunnel described in Reference 5. The tunnel draws ambient air through three inches of honeycomb and a screen into a 9 to 1 square bell contraction cone. The inlet area is 15 x 15 feet and contracts to a 5 x 5 foot square test section, that is 22 feet long.

After flowing through the contraction cone and the test section, the air then passes through a set of louvers and transitions to a circular duct. Behind the louvers in the circular duct is the fan and motor used to drive the tunnel. The fan has variable pitch blades, which are used to control the tunnel velocity. Next, the exhaust air is turned 90 degrees upward, where it is vented to the outside atmosphere.

The roof and sides of the tunnel have a variety of plexiglass windows, ranging from (12 x 18) inches to over

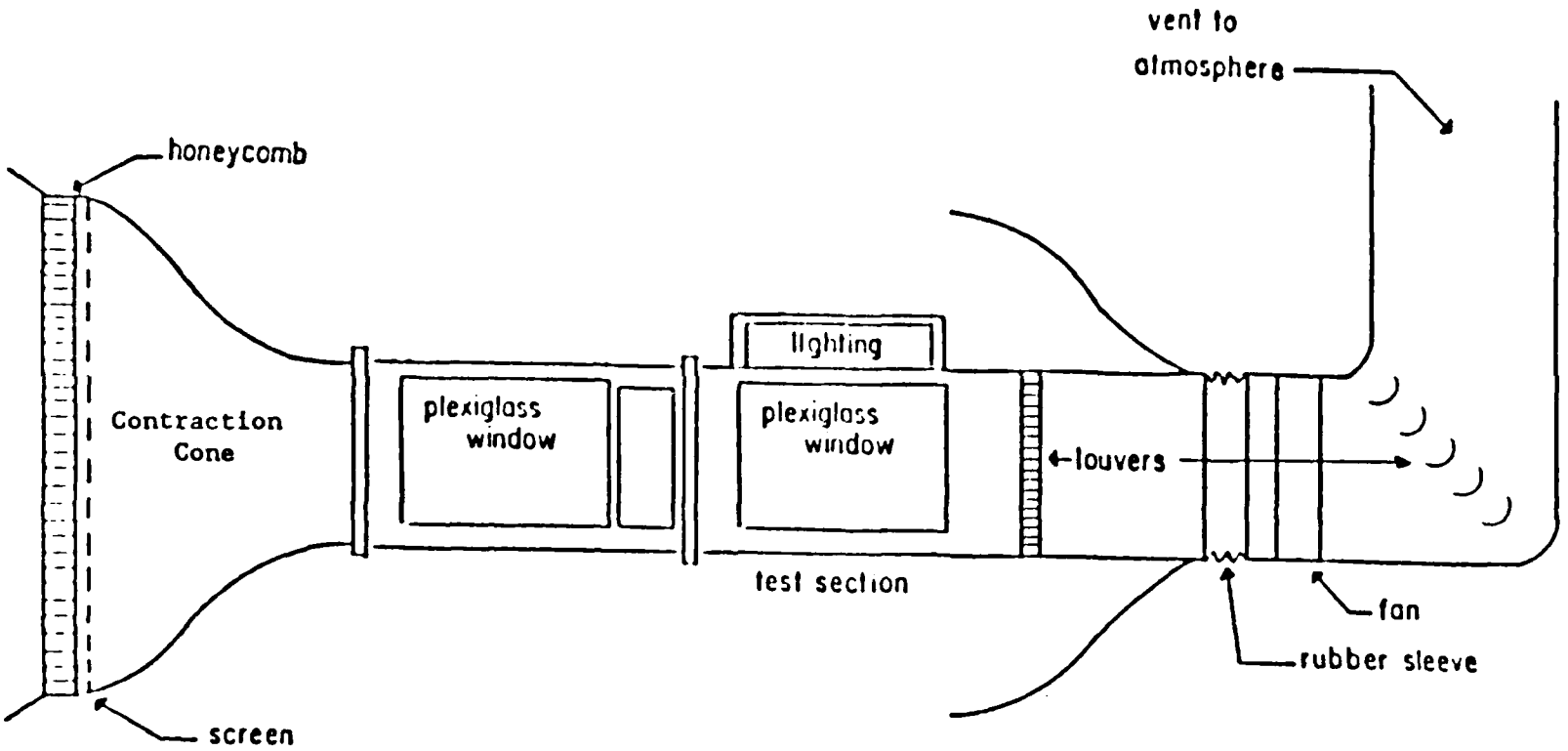

Schematic of the Naval Postgraduate
School Flow Visualization Tunnel

Figure 1

(4 x 4) feet, which are used for viewing, lighting, and photographing models in the test section. To improve the photographic contrast, the interior of the tunnel is painted with low reflective flat black paint.

2. Wind Tunnel Modifications

The initial measurements of air flow within the tunnel indicated that the velocity profile was almost uniform and the turbulence was below 1%, neither of which remotely modeled the ABL. In order to simulate the ABL, a variation of Counihan's work in of Reference 3 was used.

At the front of the test section, four 30 inch high vortex generators were installed as shown in Figure 2. To initially simulate the ABL velocity profile, the number of vortex generators was varied from three to eight. During this phase, it was confirmed that the exponential value of 'n' in equation (2) is a strong function of the number of vortex generators. As a result, Power Law Profiles with 'n' varying from .10 to .30 were obtainable.

Experimentally, it was found that the desired vertical profile was straight-forward to match for the larger n values. However, as the generators were spaced out, the horizontal profile was not as uniform as required. As a modification to Counihan's method, between the vortex generators, three 30-inch high, 2-inch diameter tapered cones were added. Without the cones, a horizontal scan of the velocity profile at the test point indicated small jets, of

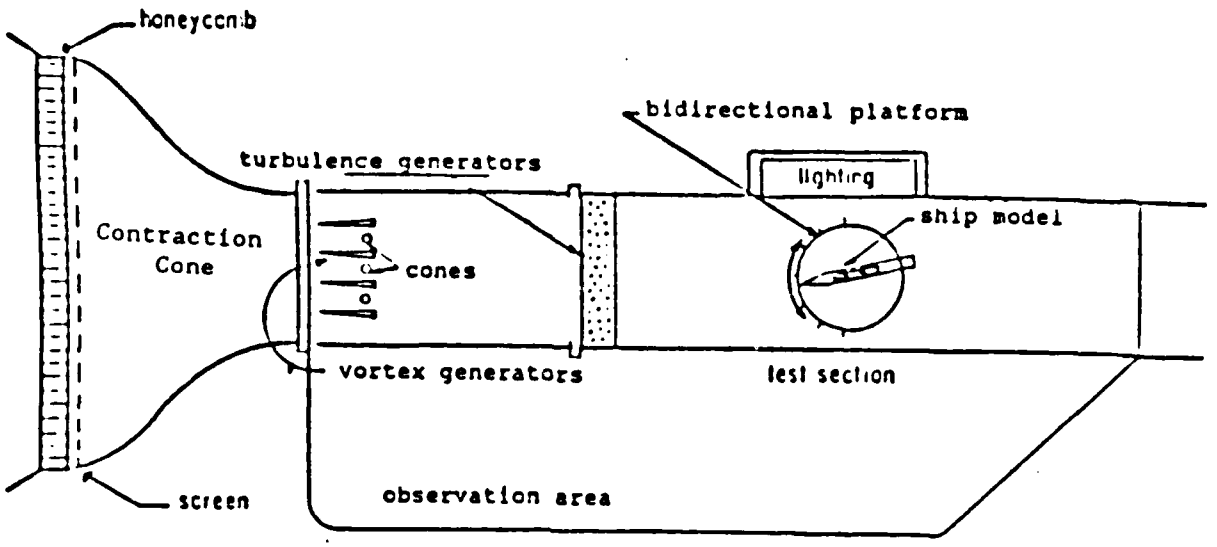

Plan View of the NPS Flow Visualization Tunnel

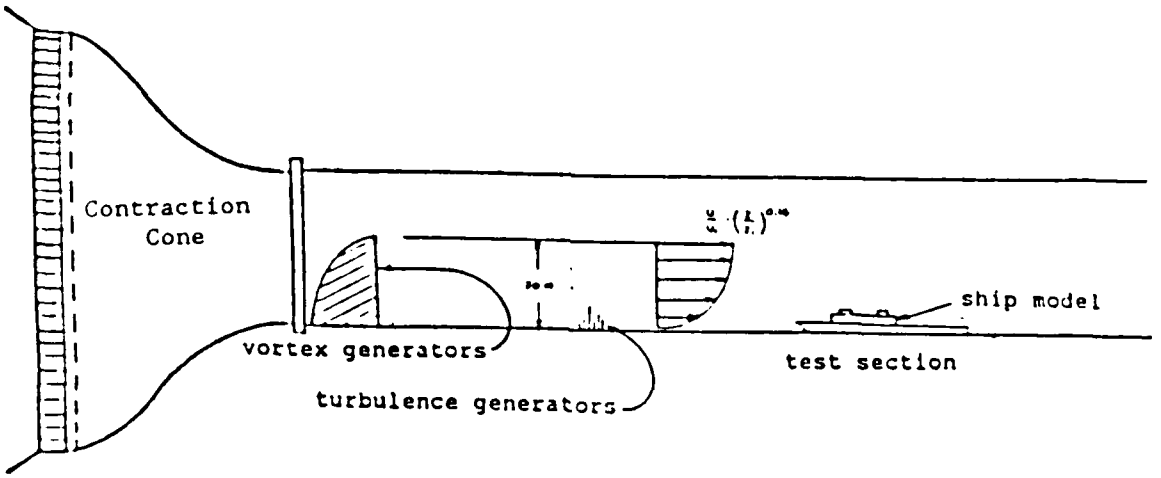

Elevation of the NPS Flow Visualization Tunnel

Figure 2

approximately 10% greater than the mean velocity, were flowing between the vortex generators.

Once the velocity profile was found to match vertically the Power Law Profile and to be uniform horizontally, then the turbulence problem was addressed. To increase the turbulence, various lengths (1-6 inches) of 3/8-inch dowels were placed randomly in a 18-inch by 5-foot rectangular section on the floor of the tunnel forward of the test section. These dowels provided the required mixing to bring the test section turbulence level up to approximately 12%, to more closely simulate the ABL.

3. Electronic Equipment

All velocity measurements were taken twice. The first measurement was taken with a DANTEC hotwire anemometer system using a single wire probe. Then, to cross check all values, a second reading was taken using an EDM 2500c micromanometer with a standard pitot static probe. Both the hotwire probe and the pitot static probe were mounted on the same linear positioning device to ensure the measurement by both probes were at essentially the same location in the flow. An HP 3478A digital voltmeter and a true RMS meter were used to record the steady and fluctuating single wire probe data. Additionally, an HP 85 computer was connected directly to the HP 3478A voltmeter via the HB-IB bus.

This system provided for a means of automatic data acquisition and, with a simple BASIC program, continuous processing of mean voltage and RMS voltage into mean velocity and turbulence levels. Both probes were mounted together in such a way that they could traverse the wind tunnel in either the horizontial or vertical direction.

4. Velocity Profile Measurements

As previously stated, the mean velocity profiles were made using a single wire probe and DANTEC hot wire apparatus. Samples taken from the digital voltmeter were sent to the HP 85 computer with a 1.6 mS integration time. As a result, approximately 550 samples per minute were sent for storage and processing to the HP 85 computer. Data points were taken every three inches horizontally across the test section and at 2, 3, 4, 8, 12, 16, 19, 25 and 30 inches vertically. This resulted in taking over 79,000 readings, forming 144 data points in a 54 by 30 inch cross section at the center plane of the test section. Table 1 is a compilation of the actual data point readings, with the mean and standard deviations included.

The velocity profile was then computed by using the average mean velocity at each elevation as the probes traversed the test section from the floor to the top of the boundary layer. Velocity profiles were then compared at two axial locations within the test section to ensure the desired degree of uniformity within the simulated ABL flow.

TABLE 1

TEST SECTION VELOCITY DATA (ft/sec)

	Z- Height above floor (inches)								
X*	2.00	3.00	4.00	8.00	12.00	16.00	19.00	25.00	30.00
6.00	6.21	6.36	6.63	7.81	7.84	8.13	8.44	8.61	9.15
9.00	6.32	6.35	6.84	7.89	7.78	8.00	8.40	8.60	9.23
12.00	6.24	6.40	6.88	7.83	7.80	8.09	8.37	8.65	9.16
15.00	6.29	6.39	6.78	7.65	7.88	8.25	8.40	8.65	9.21
18.00	6.23	6.41	6.58	7.53	7.90	8.17	8.41	8.43	9.07
21.00	6.34	6.43	6.70	7.80	8.05	8.16	8.53	8.59	9.27
24.00	6.30	6.13	6.74	7.79	8.01	8.09	8.49	8.51	9.24
27.00	6.28	6.26	6.85	7.77	7.96	8.05	8.41	8.60	9.01
30.00	6.24	6.22	6.77	7.85	7.89	8.01	8.28	8.58	9.21
33.00	6.22	6.30	6.65	7.79	7.84	7.98	8.38	8.56	8.96
36.00	6.31	6.10	6.71	7.56	7.78	8.06	8.43	8.64	8.91
39.00	6.29	6.17	6.74	7.66	7.80	8.09	8.44	8.59	9.21
42.00	6.26	6.20	6.72	7.76	7.82	8.07	8.34	8.57	8.98
45.00	6.33	6.37	6.83	7.76	7.85	8.06	8.34	8.63	9.03
48.00	6.25	6.34	6.73	7.84	7.95	8.27	8.38	8.64	8.83
51.00	6.25	6.27	6.79	7.77	8.01	8.24	8.44	8.77	9.08
AVE.	6.27	6.29	6.75	7.75	7.89	8.11	8.41	8.60	9.10
V/Vo	0.68	0.69	0.74	0.85	0.87	0.89	0.92	0.95	1.00
SIGMA	0.04	0.09	0.08	0.09	0.08	0.08	0.06	0.07	0.13

Vo at 30 inches = 9.1 ft/sec
* transverse position from far wall in inches

The resulting experimental velocity profile, along with the power law profile for n=0.11, n=0.139, n=0.20, are plotted in Figure 3. As can be seen from this figure, all but one data point fell between the two outside power law curves. This fact was confirmed by using statistical analysis of the data and a least squares fit, which indicated a power law profile with n=.139 and with a regression coefficient of .933.

5. Turbulence Measurements

When the inertia forces acting on the fluid particles are sufficiently larger than the viscous forces, the flow becomes turbulent. As pointed out in Reference 1, this is almost always the case in the ABL. Most of the time in fluid dynamics, turbulence is related to a critical Reynolds number (R crit). Then, if the associated Reynolds number of the fluid is greater than the critical Reynolds number, the motion within the fluid is said to be turbulent.

The instantaneous velocity vector V(u,v,w) in a turbulent flow will differ from the mean velocity vector $\overline{V}(\overline{u},\overline{v},\overline{w})$ in both magnitude and direction by the fluctuation vector $V'(u',v',w')$. In the ABL, the longitudinal direction is the most significant and is taken as the X direction. Therefore, the longitudinal velocity component at any instant is $u = \overline{u} + u'$. The values of the fluctuation of V' will vary ramdomly as a function of time about the mean

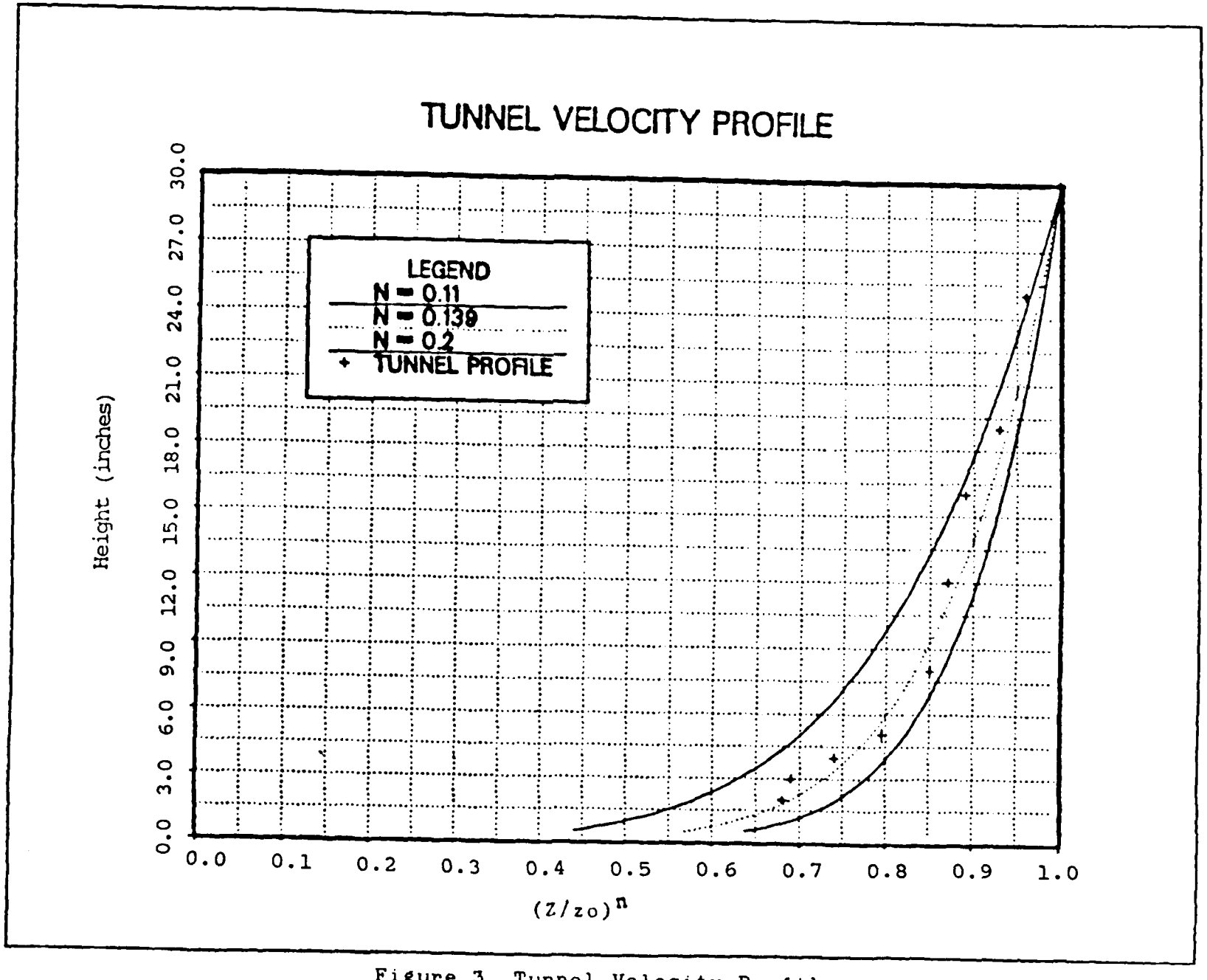

Figure 3 Tunnel Velocity Profile

value u, as shown in Figure 4, and about zero for the Y and Z components.

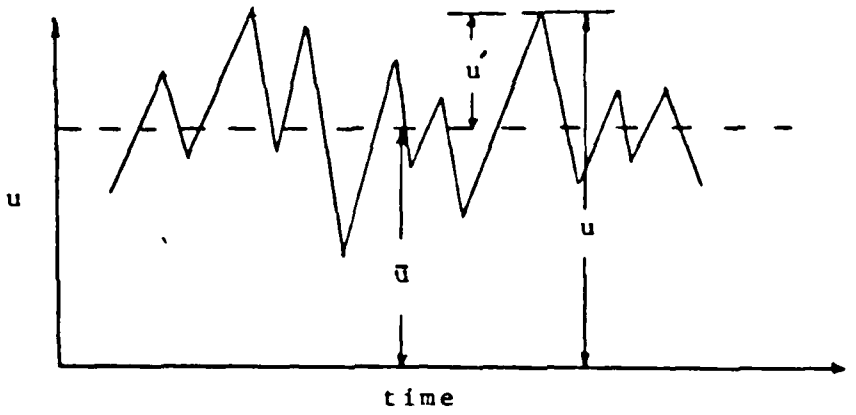

Turbulence

Figure 4

As mentioned in Section I, turbulence intensity of the flow in the longitudinal direction is defined as the RMS(u) divided by the mean velocity. This calulation was performed by the HP 85 computer, with the results seen in Table 2.

The turbulence intensity for the wind tunnel test section flow was then graphically compared to the published data of the ESDU in Reference 6, which resulted in the Figure 5 graph. As can be seen from this figure, in the region of greatest interest (below eight inches), the simulated ABL turbulence intensities compared quite favorably with the ESDU data. The weakening of the turbulence at

TABLE 2

TEST SECTION % TURBULENCE INTENSITY DATA

	Z- Height above floor (inches)								
X*	2.00	3.00	4.00	8.00	12.00	16.00	19.00	25.00	30.00
6.00	11.57	12.22	13.73	3.80	3.90	3.80	3.00	3.10	1.90
9.00	11.34	11.21	11.80	3.81	3.80	3.40	2.80	2.90	1.20
12.00	12.39	13.70	11.67	3.73	3.60	3.70	3.20	2.90	1.60
15.00	12.83	12.79	10.05	4.09	3.70	3.60	3.10	3.30	1.80
18.00	12.25	13.41	11.34	4.06	4.20	4.20	3.30	4.10	3.00
21.00	11.00	13.83	8.90	5.20	3.80	3.80	3.60	2.90	2.11
24.00	11.27	12.70	12.78	6.07	4.00	3.80	3.50	3.70	1.80
27.00	11.21	10.84	10.16	5.59	3.80	3.60	3.50	3.10	2.40
30.00	11.68	12.72	11.71	4.53	3.77	3.40	2.90	2.80	1.90
33.00	11.77	11.03	11.07	5.05	3.90	3.60	2.70	2.80	2.50
36.00	11.41	11.58	9.38	6.21	4.30	3.60	3.20	3.30	2.70
39.00	12.26	11.33	9.58	5.55	4.50	3.90	3.40	3.60	2.30
42.00	12.74	12.09	12.75	4.70	3.80	3.67	3.30	3.40	2.80
45.00	12.09	12.11	10.96	4.80	3.90	3.50	3.60	3.20	2.50
48.00	12.47	12.76	12.48	4.70	3.80	3.60	2.90	2.70	2.40
53.00	11.26	12.67	12.98	4.80	4.00	3.50	3.90	3.10	2.20
AVE.	11.85	12.32	11.33	4.79	3.92	3.66	3.24	3.18	2.19
SIGMA	0.56	0.90	1.37	0.76	0.22	0.19	0.33	0.37	0.47

Vo at 30 inches = 9.1 ft/sec

* transverse position from far wall in inches

TUNNEL % TURBULENCE

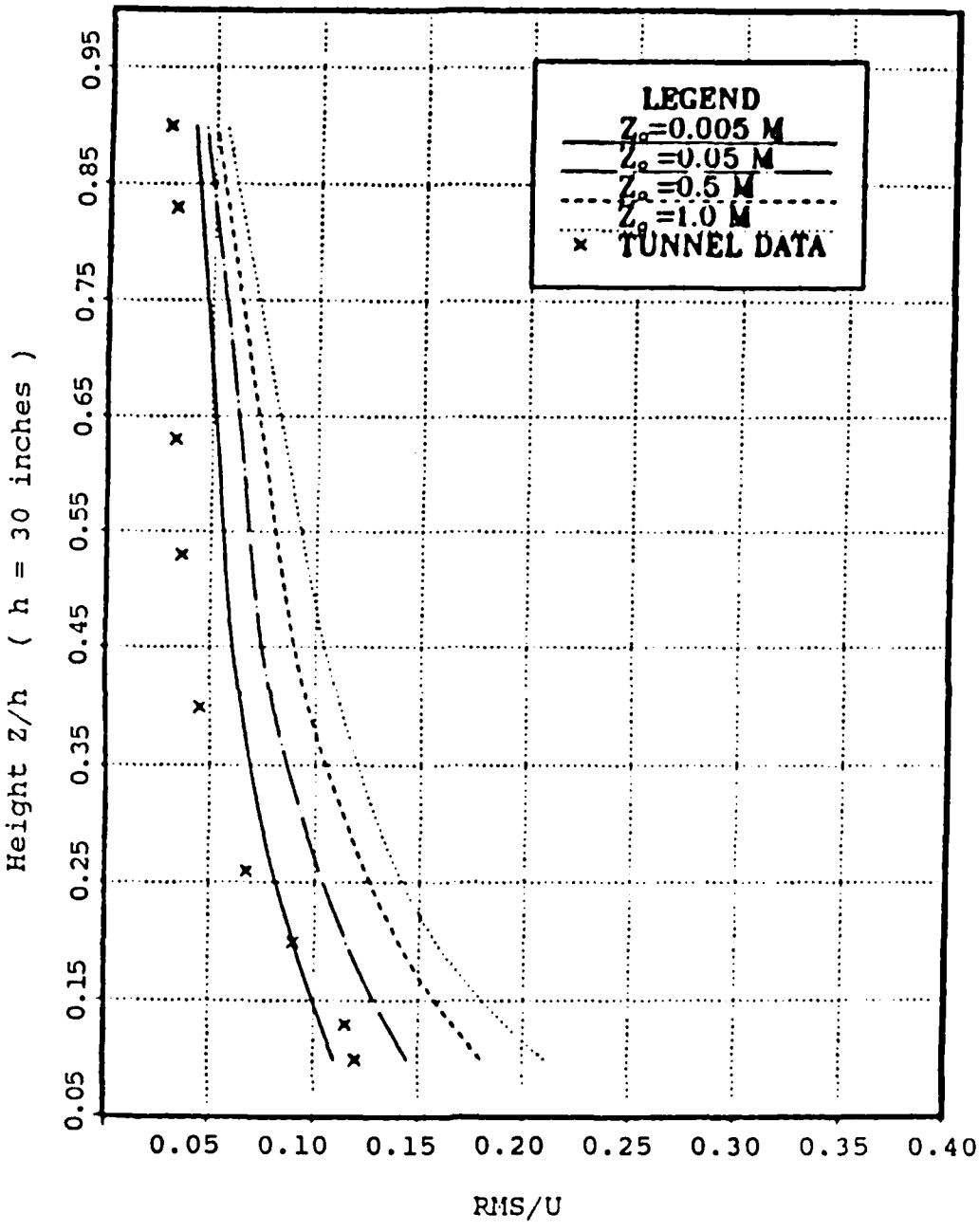

Tunnel % Turbulence
Figure 5

higher elevations was to be expected, considering the type of turbulence generators used.

C. RESULTS AND CONCLUSIONS

The flow measurements obtained in Tables (1 & 2) were taken with a free stream velocity of 9.1 feet per second at 30 inches above the test section floor. The mean velocity profile and turbulence intensities were both found to closely approximate the published data on the ABL. With these two key parameters showing such excellent agreement with References 2 and 6, and longitudinal homegeneity over the area of interest in the test section, the simulated ABL was considered to be adequate for the initial flow visualization studies.

At this point, the linear positioning device and hot wire probe were removed from the tunnel to make room for the ship model and to ease its rotation. The free-stream pitot-static system and micromanometer were left in place to monitor the tunnel V_∞ and to make any fine adjustments required to maintain 9.1 feet per second flow.

III. HELIUM BUBBLE FLOW VISUALIZATION TECHNIQUE

Helium bubble flow visualization was the technique used for the off-body flow visualization study. The basic idea behind the technique is to introduce a neutral density particle into the flow, which can then be traced as it follows a given streamline.

There are two important reasons that helium bubbles are ideal particles for use in a turbulent ABL. First, they can exist in moderate turbulence without overly dispersing. Secondly, they are large enough to be individually photographed. Thus, tracing individual streamlines is possible.

A. HELIUM BUBBLE SYSTEM

The helium bubble system used in this study was a Sage Action Inc. System, which consisted of a bubble generator console, a low speed bubble ejector head, and a neutral density bubble centrifuge. The bubble size, density, and rate of generation were controlled by adjusting the helium and bubble solution at the console. Small bubbles of about 1/8-inch diameter were generated in the head at a rate of up to 500 bubbles per second.

According to Reference 7, neutrally buoyant bubbles are usually generated at near maximum helium flow rates. This was found to be true. However, in practice, it was found to

be extremely difficult to maintain this precise mixture of helium and bubble solution. Since it was critical to use neutrally buoyant bubbles in order to faithfully trace the flow, a neutral density bubble centrifuge was added in series with the console and ejector head.

The centrifuge allowed for a much larger range of mixtures of the helium and bubble solution. And, by design, the centrifuge sorted out the light and heavy bubbles, thus insuring that only neutrally buoyant bubbles were allowed to leave the unit. After leaving the centrifuge, the neutrally buoyant bubbles passed through six feet of 3/8-inch inner diameter plastic pipe and entered the flow approximately 18 inches upstream from the model.

B. LIGHTING

Because of the small size and low reflectivity of the bubbles, careful selection of the light sources and extreme care in their placement was required. The initial lighting set-up was patterned after, and was quite similar to, the one suggested by Mueller in Reference 8. Well downstream from the model and outside the tunnel, high intensity lights were arranged so that narrow beams of light were directed upstream and across the model, illuminating the bubbles.

Even with low reflective black paint on all surfaces of the tunnel and model, the lighting still proved to be a real challenge. Compounding the normal problems associated with

this type of lighting was the fact the model was three dimensional and irregularly shaped, so that it too required enough light to make it visible. This final lighting problem was solved by using a low 75-watt source above the tunnel, giving faint background light to the entire test section and model.

C. PHOTOGRAPHY

Due to the very low light conditions and time exposure requirements, bubble trace photography is quite different from conventional photography. To optimize the streamline visualization, it is desirable to obtain a high trace intensity with a low background exposure.

Trying to obtain this optimization again proved to be a real challenge. Color film with ASA's of 400, 1000, and 1600 and black-and-white film with ASA's of 400 and 3000 were all evaluated with various 'f' stops to determine the best combination.

For this study, the most consistent results were produced with Kodak T-Max 400 professional film, which was then pushed two stops to 1600 ASA.

IV. FLUORESCENT MINITUFTS

For the on-body flow visualization portion of the study, an ultraviolet fluorescent minituft system was used. The basic idea behind this technique is to secure one end of extremely thin fluorescent nylon monofilament minitufts to the surface of the model. These minitufts will, under flow conditions, align themselves in the direction of the local streamlines. Because of the fragility of the tuft fibers, thousands of minitufts can be applied to various surfaces of the model and the tunnel floor without disrupting the flow field.

Next, to visually record the local streamlines, a high powered ultraviolet light source was used to excite the minitufts for fluorescent photography.

A. MINITUFTS

The minitufts used in the study were made of .0007-inch diameter fluorescent nylon monofilament. The system used was adapted from the system described by Crowder in Reference 9.

The minitufts themselves were 0.5 inches in length and were evenly spaced on a grid 0.25 inches across and 0.50 inches lengthwise on the model. They were secured at their forward end with a small drop of cyanoacylate adhesive

(super glue). The adhesive was thin and penetrated into the wooden surface of the model nicely, leaving virtually no surface disruption. Although precautions had to be taken with this type of adhesive, the results were well worth it. As it turned out, the minitufts were secured well enough to withstand direct applications of a high speed jet of air, with pressure from a 50 psi source, without detaching.

After the adhesive cured, each tuft was then cut to length and the free end lifted off the surface by brushing and using a jet of compressed air. This procedure was performed to ensure there were no residual cantilevered forces, from the adhesive, holding the minituft in a pre-determined direction.

B. FLUORESCENT PHOTOGRAPHY

Successful fluorescent photography is a function of the type of ultraviolet light source, the filters used on the light source and camera, and type of film. The ultraviolet light causes the fluorescent minitufts to re-radiate at a wavelength determined by the chemical used to dye the minitufts.

Actual ultraviolet light, which has a wavelength below 400 nanometers, is invisible to the eye, but can be detected photographically since photographic materials are inherently sensitive to it. Fortunately, the minitufts re-radiated fluorescence in the low end of the visible spectrum, easing

the mechanics of taking pictures. Because the fluorescence is much weaker than the reflected ultraviolet radiation and normal background light, special Kodak Wratten filters were used over the camera lens to filter out much of the UV light, transmitting most of the fluorescence from the minitufts.

Fluorescent tubes (black lights), designed especially to emit long-wave ultraviolet light, were used as the UV source. The glass of the tubes contained filter material, which is opaque to most visible light, but freely transmits the long wave UV light.

For the actual photography, color film with ASA's of 400 and 1000, and black-and-white film with ASA's of 400 and 3000 were evaluated with various 'f' stops. Again, for this low light condition, the most consistent results were obtained with Kodak T-Max 400 professional film that was pushed to 1600 ASA.

V. RESULTS

The helium bubble and fluorescent minituft flow visualization techniques have been described in detail. For the actual photographs, yaw angles of 0 , 15 , 30 , and -30 degrees were selected. In the following figures, direct comparisons of the two methods are made at each of the four yaw angles. It should be noted that these pictures are, in many cases, the best of numerous photographs taken with different lighting, "f" stops, and exposure times. As previously mentioned, the lighting for the photography is indeed the most difficult area to master in flow visualization.

In order to facilitate the discussion and comments on the various photographs the following definitions are used;

i) The superstructure refers to the large block above the hull of the ship model.

ii) The forward and aft blocks refer to the smaller rectangular blocks located on top of the superstructure.

iii) The top of the hull is the first level.

iv) The top of the superstructure is the second level.

The tunnel V_∞ was measured at 30 inches and held constant at 9.1 feet per second for all of the test runs. Using equation (2) or the data from Table 1, the freestream

velocity can be computed for the various heights of interest. The velocity at the first level (z = 2 inches) was approximately 6.25 feet per second; at the second level (z = 3.5 inches), approximately 6.55 feet per second; and at the top of the blocks (z = 4.50 inches), approximately 6.9 feet per second.

A. ZERO DEGREE YAW

Figures 6a - 8b show that, for the zero degree yaw case, even in a turbulent ABL, the overall flow appears relatively smooth and quite symmetrical. The most significant trailing vortices come from the trailing edge of the superstructure and blocks on the second level. The flow coming over the bow apparently re-attaches quite near the edge of the bow, as there is no evidence of detached flow on the forward portion of the first level. The flow coming over the bow then separates as it flows around the forward portion of the superstructure.

On the second level, prior to the forward block, a foot vortex is present, as shown by the lifting tufts and helium bubble vortex. The vortex behind the superstructure on the first level appears to be fairly weak at this point.

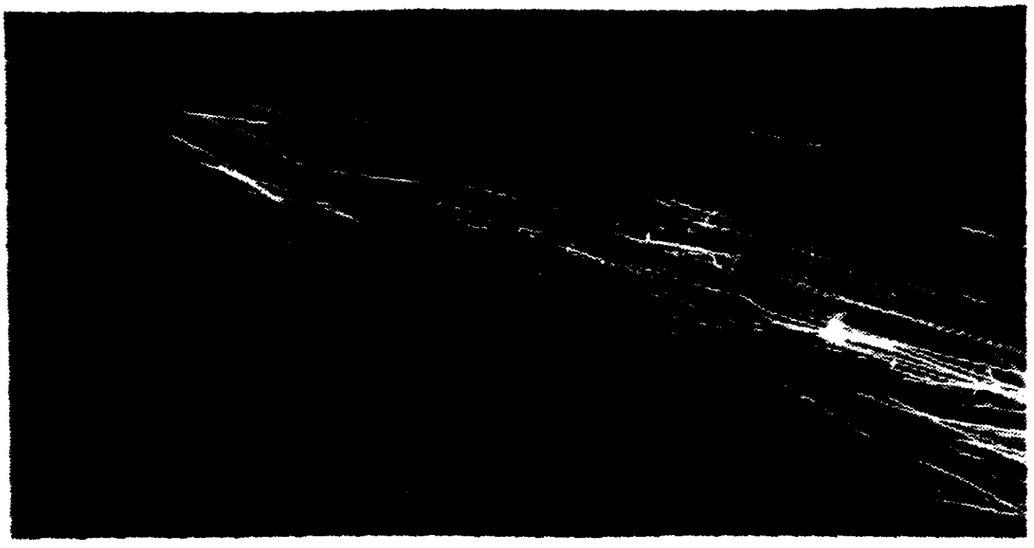

Figure 6a

0 Degree Yaw with Helium Bubbles of the Bow

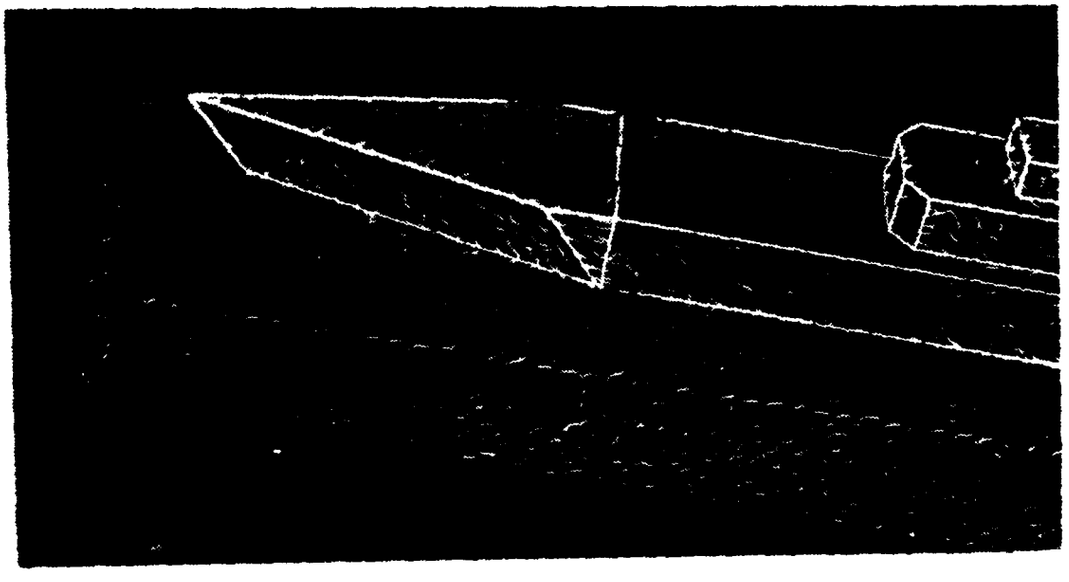

Figure 6b

0 Degree Yaw with Minitufts of the Bow

Figure 7a

0 Degree Yaw with Helium Bubbles of midships

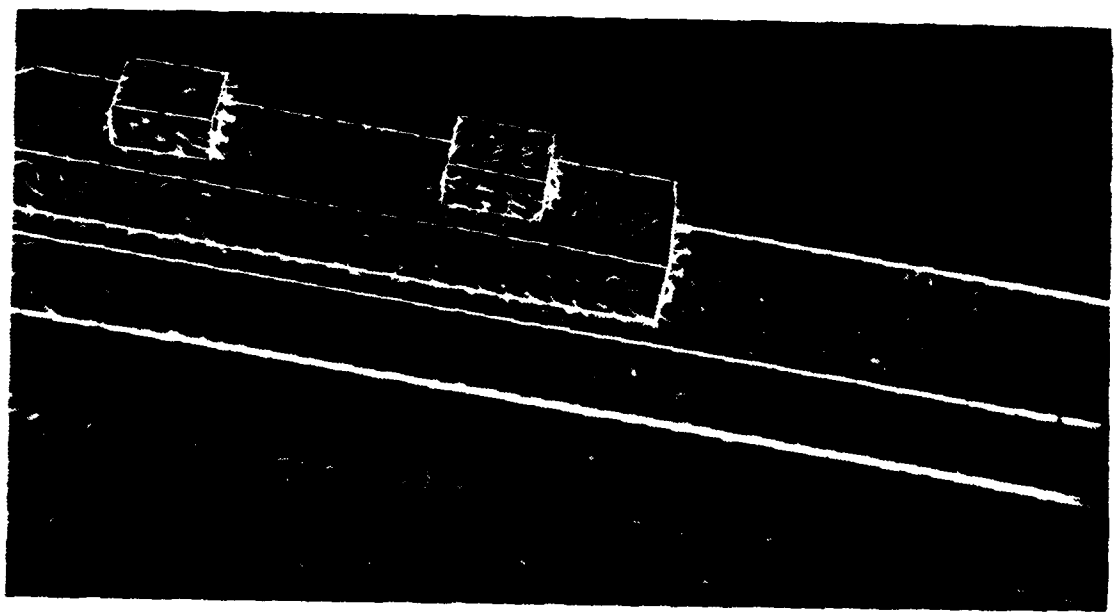

Figure 7b

0 Degree Yaw with Minitufts of midships

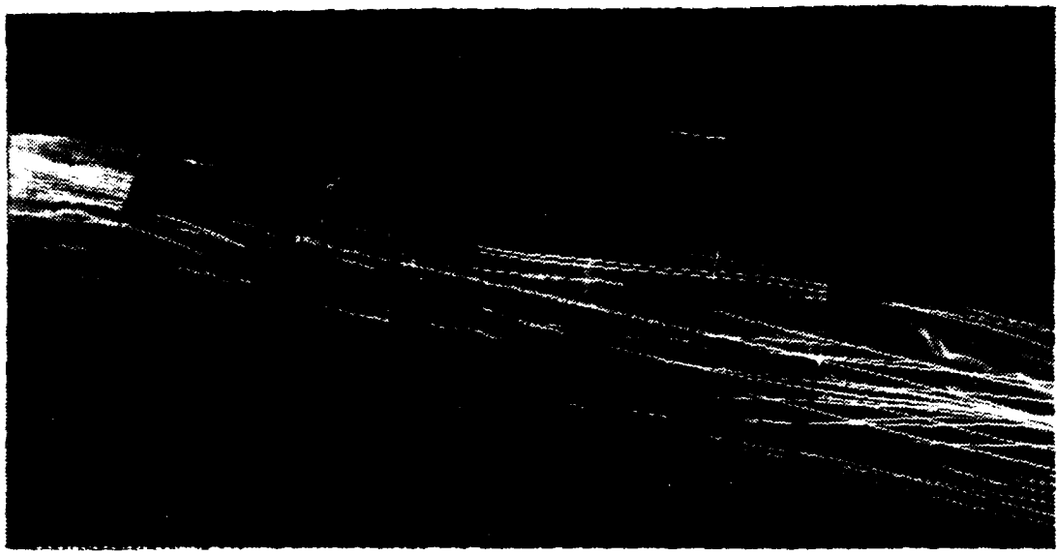

Figure 8a

0 Degree Yaw with Helium Bubbles of the Ship

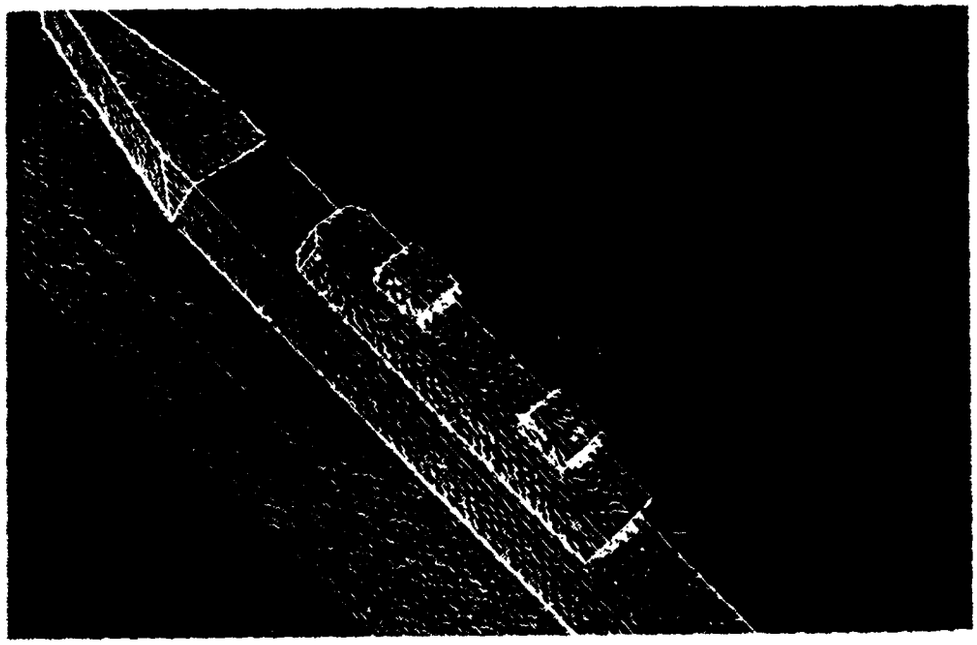

Figure 8b

0 Degree Yaw with Minitufts of the Ship

B. FIFTEEN DEGREES STARBOARD YAW

For the fifteen degrees right yaw case, Figures 9a - 11b clearly show the overall flow to be more disturbed than in the zero degree case. Additionally, the trailing vortex structure is no longer symmetrical, and the leeward (downwind) side appears to have much stronger activity.

The corners on the leeward side, of the superstructure and blocks, are now producing the dominant trailing vortices. These vortices are then pulled down and combine on the downwind side of the ship and start forming a large corkscrew vortex. The activity in the near wake, just aft of the superstructure, is apparently strengthening and is more easily identified. The flow coming over the bow is no longer re-attaching next to the edge. The mean re-attachment line there has moved inboard and is starting a small vortex of its own.

Figure 9a

15 Degree Yaw with Helium Bubbles of the Bow

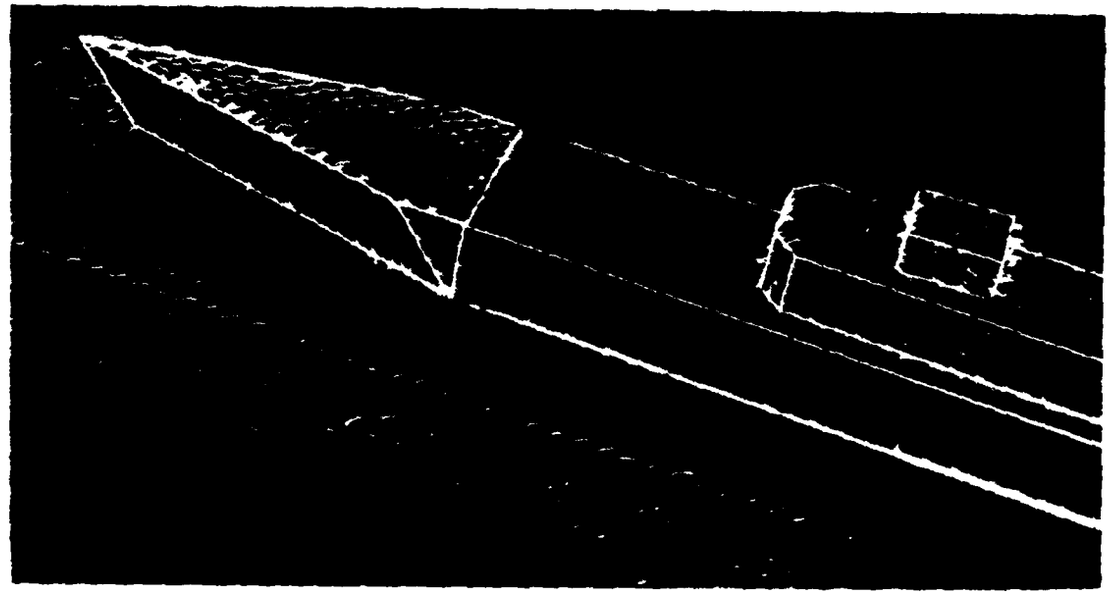

Figure 9b

15 Degree Yaw with Minitufts of the Bow

Figure 10a

15 Degree Yaw with Helium Bubbles of midships

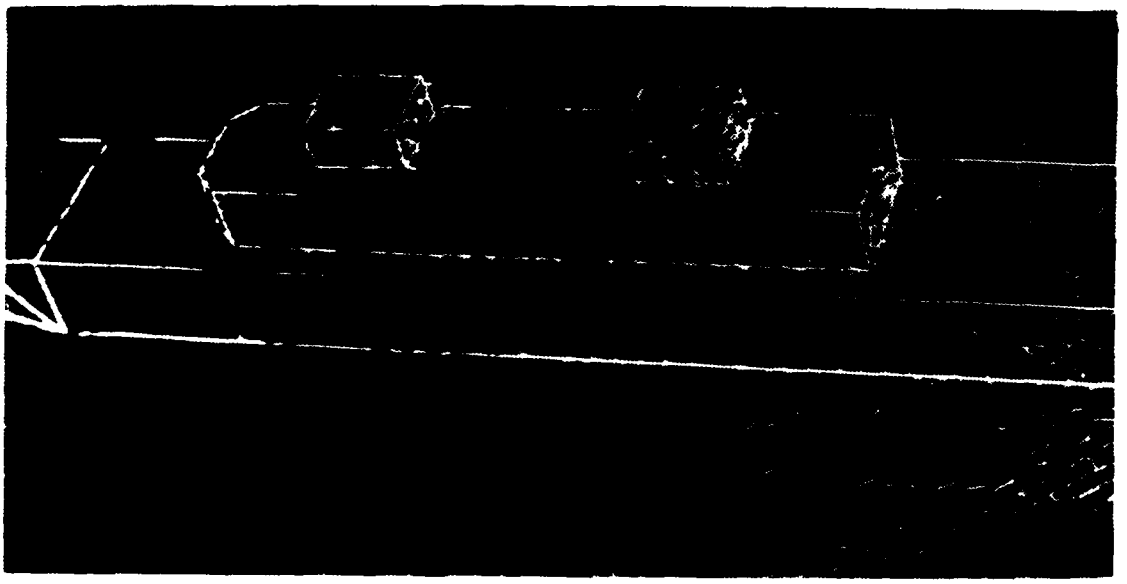

Figure 10b

15 Degree Yaw with Minitufts of midships

Figure 11a

15 Degree Yaw with Helium Bubbles of the Ship

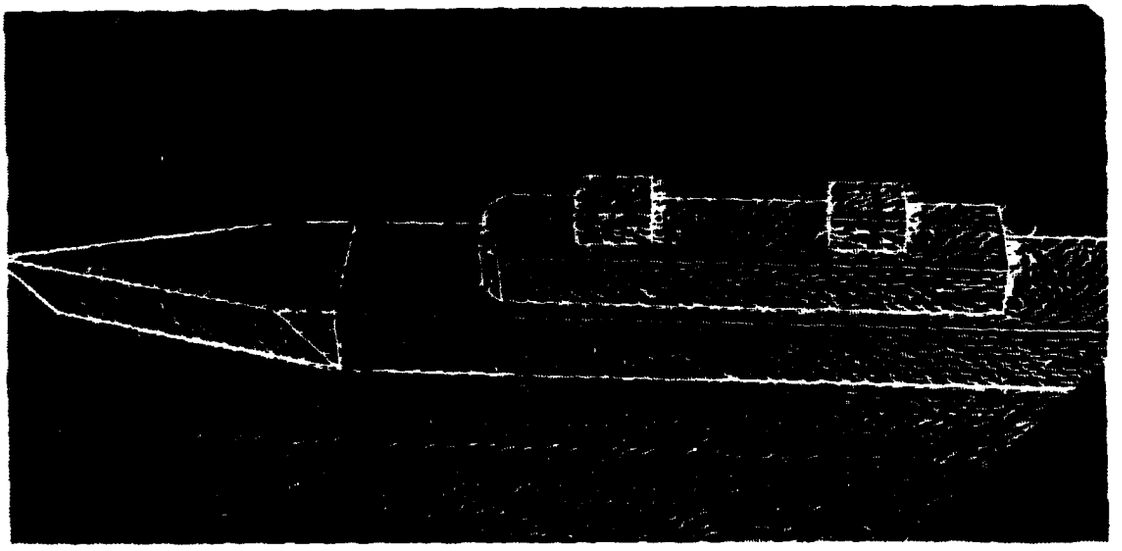

Figure 11b

15 Degree Yaw with Minitufts of the Ship

C. THIRTY DEGREES STARBOARD YAW

In Figures 12a - 14b, one can now see the flow is even more disrupted than in either of the previous cases. The vortices have all apparently increased in strength.

The vortices, from the trailing corner of the superstructure and trailing corners of the blocks, no longer appear to dominate the flow as they did in the fifteen degree case. The trailing vortices again combine to produce an even stronger corkscrew vortex on the downwind side of the ship. However, due to the increased yaw angle, the corkscrew vortex has shifted slightly away from the ship.

The area, behind and close to the superstructure on the first level, is now clearly in a much more turbulent flow. The flow over the bow appears to have separated and re-attached while continuing to develop a vortex of its own.

Figure 12a

30 Degree Yaw with Helium Bubbles of the Bow

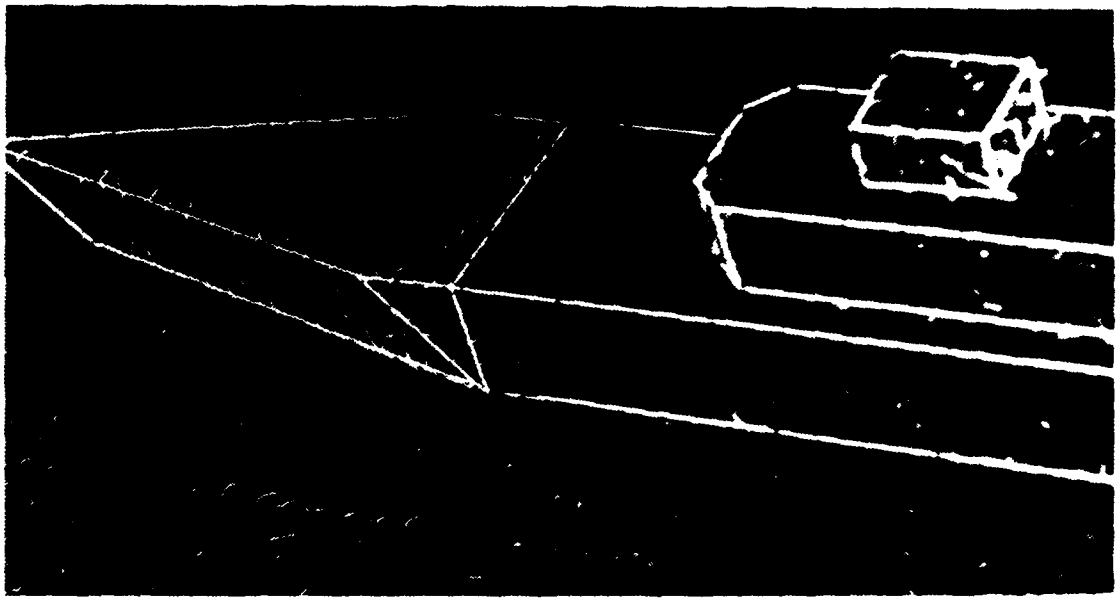

Figure 12b

30 Degree Yaw with Minitufts of the Bow

Figure 13a

30 Degree Yaw with Helium Bubbles of midships

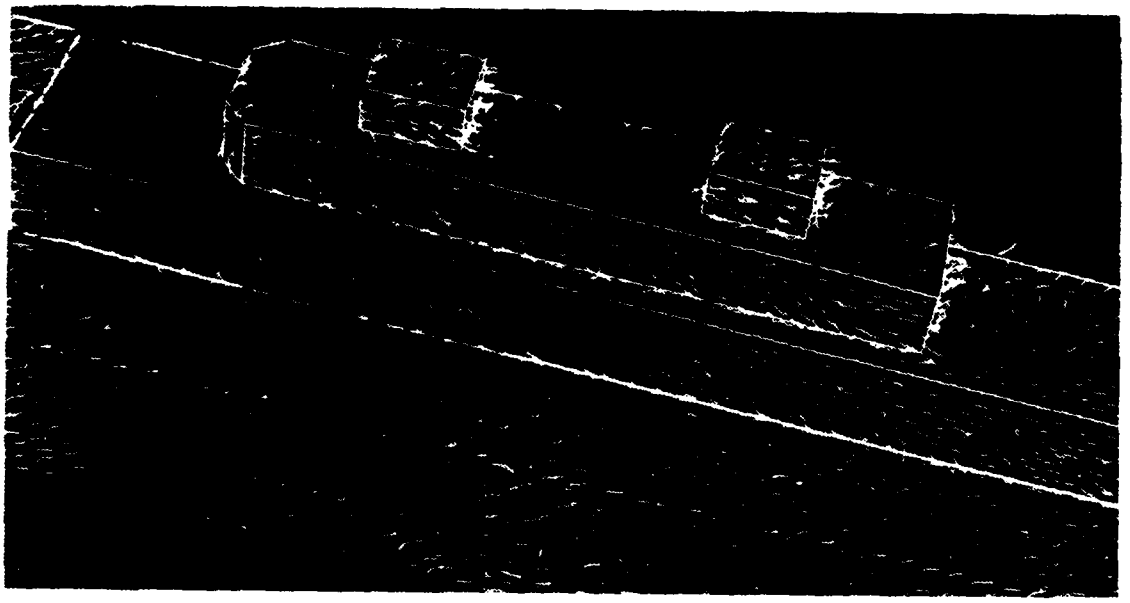

Figure 13b

30 Degree Yaw with Minitufts of midships

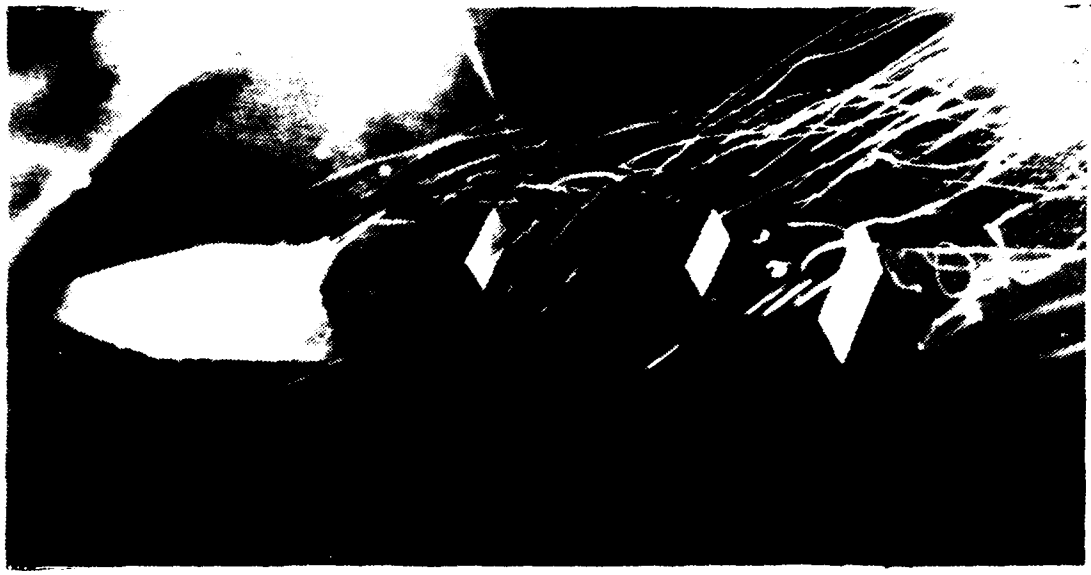

Figure 14a

30 Degree Yaw with Helium Bubbles of the Ship

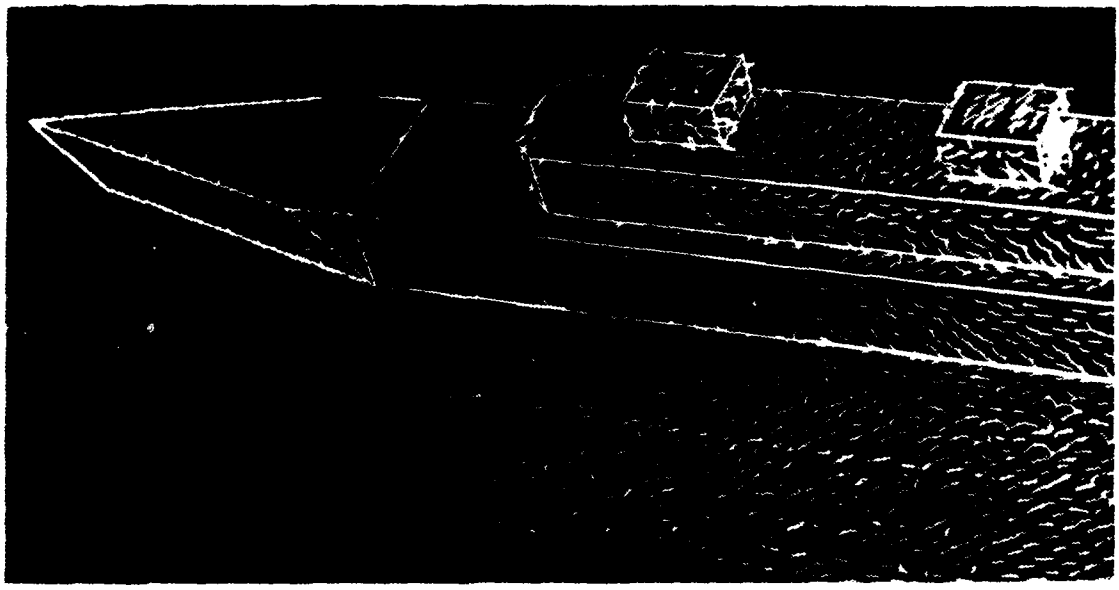

Figure 14b

30 Degree Yaw with Minitufts of the Ship

D. THIRTY DEGREES PORT YAW

As expected, Figures 15a - 17b show the thirty degrees port-yaw case to be approximately the mirror image of the thirty degrees starboard case. These figures graphically depict the strong trailing vortices of the port side superstructure and block corners.

From this view, the pull-down of the flow over the model is more apparent, as is the strong corkscrew vortex on the lee side. The area behind and close to the superstructure on the first level again shows a region of highly turbulent flow.

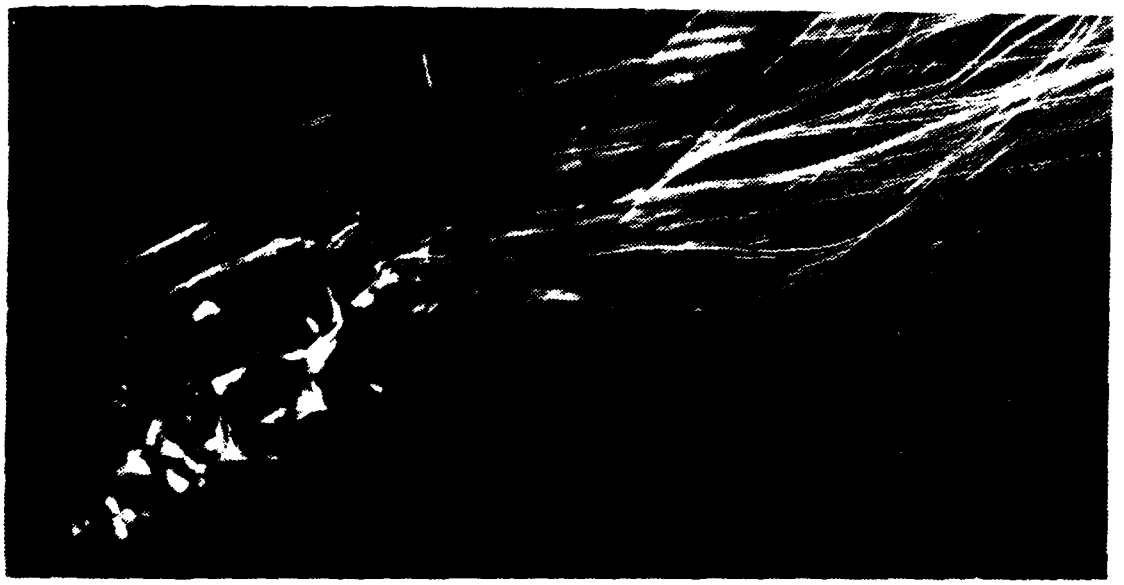

Figure 15a

-30 Degree Yaw with Helium Bubbles of the Bow

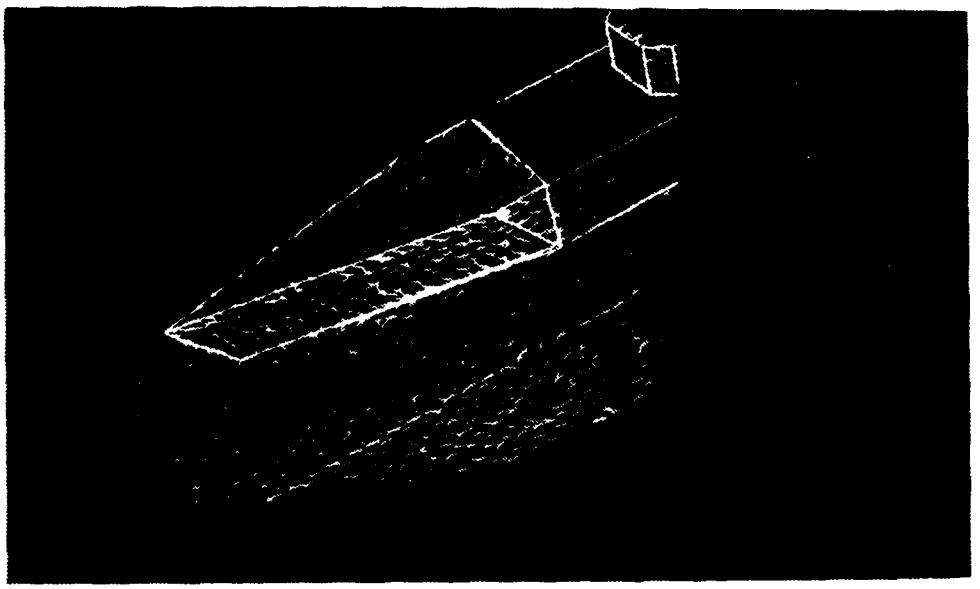

Figure 15b

-30 Degree Yaw with Minitufts of the Bow

Figure 16a

-30 Degree Yaw with Helium Bubbles of midships

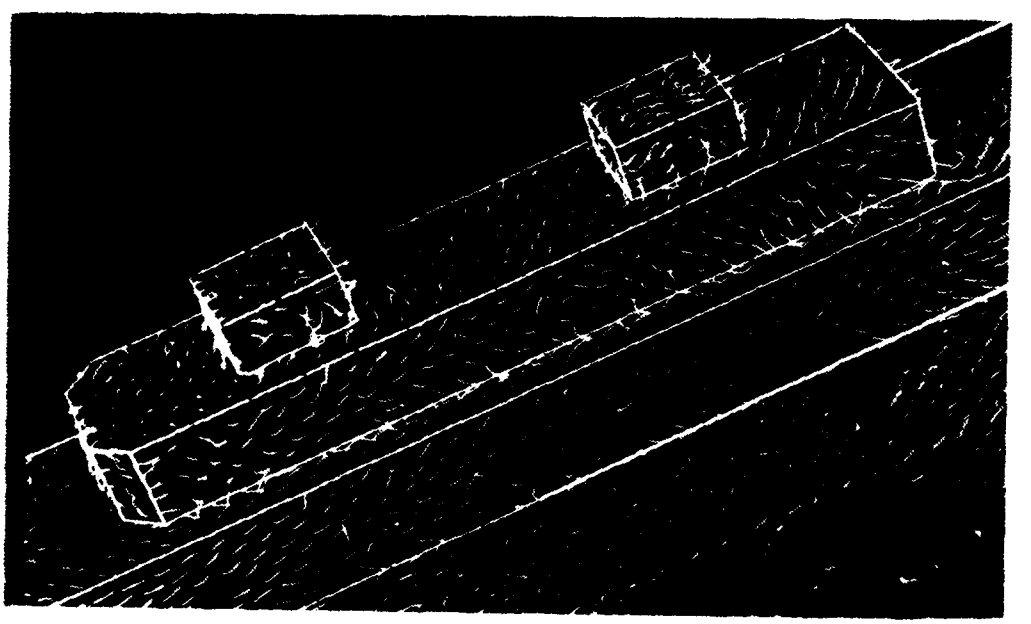

Figure 16b

-30 Degree Yaw with Minitufts of midships

VI. CONCLUSIONS AND RECOMMENDATIONS

This paper was concerned with an experimental investigation of a simulated turbulent atmospheric boundary layer around a generic destroyer model using two flow visualization techniques. As a result of the study some basic conclusions can be drawn.

1) A viable neutral-density stable atmospheric boundary layer was simulated in the NPS low-speed wind tunnel.
2) The helium-bubble apparatus functioned well but, better lighting is essential for high-quality photography.
3) The ultraviolet lighting/fluorescent minituft technique was very successful and less demanding photography-wise, as the lighting required little adjustment for the different yaw angles.
4) A detailed study of turbulent ABL flow around ship models is possible in the NPS Low Speed Wind Tunnel.

In order to futher expand the productivity of this facility for future investigations, the following recommendations are made.

1) Even though the lighting for the helium bubble technique was adequate for this study, it was too cumbersome and time consuming to be used continuously for

follow-on work; better overall lighting should be considered.

2) To reduce the glare and distortion problems, all plexiglass observation windows should be replaced with a high quality shatterproof non-relective glass.

3) Frequently, the observation room was found to be too small for the required camera equipment. This room needs to be expanded in size, include both sides of the tunnel and isolated from the tunnel vibrations to expedite equipment set-up and improve photograph quality.

4) A further study is needed to determine the details of the area immediately aft of the superstructure, which is the normal helicopter landing area. An aerosol injection flow visualization study would probably be appropriate.

LIST OF REFERENCES

1. Healey, J. Val, "The Propects for Simulating the Helicopter/Ship Interface," Naval Engineers Journal, pp. 45-63, March 1987.

2. Arya, S. P., in Engineering Meteorology, ed., Erich J. Plate, pp. 233-267, Elsevier Scientific Publishing Company, Amsterdam, Netherlands, 1982.

3. Counihan, J., "An Improved Method of Simulating an Atmospheric Boundary Layer in a Wind Tunnel," Atmospheric Environment, v. 3, pp. 197-214, 1969.

4. Davenport, A. G., in Engineering Meteorology, ed., Erich J. Plate, Chapter 12, pp. 527-569, Elsevier Scientific Publishing Company, Amsterdam, Netherlands, 1982.

5. Naval Air Engineering Laboratory Report NAEL-ENG-6818, The Three Dimensional Smoke Tunnel of the Naval Air Engineering Laboratory in Philadelphia, Pennsylvania, by F. O. Ringleb, 10 July 1961.

6. E. S. D. U. Data Item 74031, Engineering Sciences Data Unit International, Suite 200, Chain Bridge Road, McLean, Virginia 22101.

7. Sage Action, Incorporated, SAI Bubble Generator Model 3, by R. W. Hale, P. Tan and D. E. Ordway, March 1971.

8. Mueller, T. J., in Fluid Mechanics Measurements, ed., R. J. Goldstein, Chapter 7, pp. 307-372, Hemisphere Publishing Corporation, 1983.

9. Crowder, J. P., "Add Fluorescent Minitufts to the Aerodynamicist's Bag of Tricks," Astronautics and Aeronautics, pp. 54-57, November 1980.

INITIAL DISTRIBUTION LIST

		No of Copies
1.	Defense Technical Information Center Cameron Station Alexandria, VA 22304-6145	2
2.	Library, Code 0142 Naval Postgraduate School Monterey, CA 93943-5002	2
3.	Department Chairman, Code 67 Department of Aeronautics Naval Postgraduate School Monterey, CA 93943	1
4.	Commanding Officer Naval Air Systems Command Air Vehicle Division Attn. Captain N.S. Flynn, Code Air 53 Jefferson Plaza 2, Rm 916 Washington, D.C. 20361	1
5.	Commanding Officer Naval Air Systems Command Air Vehicle Division Attn. Mr Jonah Ottensoser, Code Air 53011c Jefferson Plaza 2, Rm 904 Washington, D.C. 20361	1
6.	David Taylor Naval Ship Research and Development Center Attn. Eric Baitis, Code 1561 Bethesda, MD 20084	1
7.	Naval Research Laboratory Atmospheric Physics Division Attn. Mr Ted Blanc, Code 4110 Washington, D.C. 20375	1
8.	Naval Air Test Center Attn. Mr Dean Carico, Code RW40a Patuxent River, MD 20670	1
9.	Naval Air Test Center Attn. Mr Jerry Higman, Code RW81 Patuxent River, MD 20670	1

10. Dr J. Val Healey, Code 67He — 4
Department of Aeronautical Engineering
Naval Postgraduate School
Monterey, CA 93943

11. LCDR William K. Bolinger — 4
13380 Frinks Court
Herndon, VA 22070

12. Mr R.A. Feik — 1
Aeronautical Division
Aeronautical Research Laboratories
506 Lorimer Street
Fishermans Bend
Box 4331 P.O.
Melbourne, Vic. 3001
Australia

13. Naval Air Development Center — 1
Attn. Mr John Clarke, Code 6053
Warminster, PA 18974

END

10-87

DTIC